Remote Sensing Letters
Vol. 3, No. 3, May 2012, 267–275

Taylor & Francis
Taylor & Francis Group

A change detection measure based on a likelihood ratio and statistical properties of SAR intensity images

BOLI XIONG*†‡, JING M. CHEN‡ and GANGYAO KUANG†

†Department of Information Engineering, School of Electronic Science and Engineering, National University of Defense Technology, Changsha, Hunan, PR China

‡Department of Geography and Programming in Planning, University of Toronto, Toronto, ON, Canada

(*Received 8 September 2010; in final form 10 March 2011*)

With its weather- and illumination-independent characteristics, synthetic aperture radar (SAR) has become an important tool for change detection. There are two critical steps in SAR image change detection: designing a change detector and choosing a decision rule. Given a measure from a change detector, the change detection results could be sensitive to the decision rule, such as the selection of a threshold. This letter presents a change detection measure based on a likelihood ratio and the statistical distribution of SAR intensity images. The likelihood ratio is defined as the ratio between the joint probability density functions (PDFs) of a pair of SAR images. Under the condition that both PDFs follow the gamma distribution, the histogram of this change detection measure deduced from the likelihood ratio has a single and steep peak that can be used to reliably and easily determine the change detection threshold. Analyses of SAR image pairs from different platforms show that the proposed change detection measure is simple and effective in detecting changes.

1. Introduction

Change detection is a process of acquiring time-dependent information of objects of interest from the same scene observed at different times. Synthetic aperture radar (SAR) has been an important technique for change detection for various applications such as environmental monitoring (Wang and Allen 2008, Makkeasorn *et al.* 2009), agricultural surveys, urban studies, forest monitoring and disaster evaluation (Bovolo and Bruzzone 2007). Changes in a SAR scene are manifested mainly as differences of intensity or local texture among multi-temporal SAR images. Image differencing is one of the most widely used change detection algorithms for a variety of geographical environments (Singh 1989). Image ratioing is another change detection method which is also as simple and quick as image differencing. It is widely used in SAR image change detection because of multiplicative noise reduction when data are ratioed on a pixel-by-pixel basis. It is well known that, intrinsic to all active imaging systems, SAR images suffer from speckle noise due to coherence from distributed targets (Franceschetti and Lanari 1999). The variety of the noise and imaging conditions

*Corresponding author. Email: bolixiong@gmail.com

Remote Sensing Letters
ISSN 2150-704X print/ISSN 2150-7058 online © 2012 Taylor & Francis
http://www.tandf.co.uk/journals
DOI: 10.1080/01431161.2011.572093

in the data acquisition process affects the performance and stability of SAR change detection. In particular, a simple threshold of 0 for image differencing and 1 for image ratioing may not be appropriate to identify change from no-change. In this letter we propose a change detection measure that is based on a likelihood ratio of SAR intensity images and a theoretical analysis of SAR statistical properties. With the proposed change detection measure, one can estimate an optimum threshold that differentiates the changes from the non-changed areas.

2. The proposed change detection measure

There are two key steps in classical SAR image change detection (Inglada and Mercier 2007). First is the development of a change detection measure, and the second is to make a decision with this measure. Image differencing appears to be an appropriate measure in change detection if the data are affected by additive Gaussian noise (Coppin and Bauer 1996). However, SAR speckle is a multiplicative noise, and thus image ratioing of the multi-temporal radar intensity data is better adapted to the statistical features of SAR data than image differencing (Rignot and Zyl 1993). An alternative change detection measure widely used in SAR change detection is the log-ratio (Bazi *et al.* 2006), which converts the linear scale of SAR data to a logarithmic scale before the differencing operation, and thus transforms the multiplicative noise into additive noise.

The results after image differencing or ratioing are called 'residual data' (Jha and Unni 1994). The choice of a threshold differentiating the change from no-change in unsupervised change detection can be made automatically on the basis of residual data. The automatic selection of thresholds is of particular interest in SAR change detection (Bruzzone and Prieto 2000, Rogerson 2002, Moser and Serpico 2006). Based on the likelihood ratio and the gamma distribution of SAR intensity images, a statistical hypothesis testing is proposed for change detection of SAR data (Conradsen *et al.* 2003). With this hypothesis testing, a new change detection measure is deduced, which is not only as simple as image differencing, but also reliable and provides an easy method for selecting a threshold.

In this letter, each pixel in a SAR image is assumed to be independent of the other pixels. If x expresses the intensity value of a pixel in a homogenous region of an L-look SAR image, the probability density function (PDF) of x is (Dekker 1998, Oliver and Quegan 2004)

$$P(x) = \frac{1}{\Gamma(L)} \left(\frac{L}{u}\right)^L x^{L-1} \exp\left(-\frac{Lx}{u}\right) \tag{1}$$

where $\Gamma(\cdot)$ is a gamma function. From the moment estimation, the mean (E) and variance (D) of x are as follows:

$$E(x) = u, \;\; D(x) = \frac{u^2}{L} \tag{2}$$

It can be assumed that there are M groups of SAR images, and each group contains a SAR image after an L-look processing. Given a pixel x_{ij} in a homogenous area, which is surrounded by N-1 adjacent pixels that follow the same PDF, the joint PDF of x_{ij} ($i = 1, 2, \ldots, N$, $j = 1, 2, \ldots, M$) can be expressed as

$$P(X) = P\left(x_{11}, x_{12}, \ldots, x_{NM}\right) = \prod_{i=1}^{N}\prod_{j=1}^{M} \frac{1}{\Gamma(L)}\left(\frac{L}{u_j}\right)^{L} x_{ij}^{L-1} \exp\left(-\frac{x_{ij}L}{u_j}\right) \tag{3}$$

where u_j is the average intensity of pixels in the homogenous area of each image.

When $M = 2$, the first image is regarded as the so-called master image, and the second the slave for change detection. Using the moment estimation in equation (2), the change detection problem is addressed by using the following binary hypothesis test (Chatelain and Tourneret 2007):

$$\mathrm{H}_0 \text{ (unchanged pattern)}: u_1 = E(x_1) = u_2 = E(x_2) = u_0$$

$$\mathrm{H}_1 \text{ (changed pattern)}: u_1 = E(x_1) \neq u_2 = E(x_2)$$

where x_1 and x_2 are the pixels in the master and slave images, respectively. Combined with equation (3), the conditional probabilities in a likelihood ratio test can be described as follows:

$$\lambda_1 = P(X|\mathrm{H}_0) = \prod_{i=1}^{N} \frac{1}{\Gamma^2(L)}\left(\frac{L}{u_0}\right)^{2L} x_{i1}^{L-1} x_{i2}^{L-1} \exp\left(-\frac{L}{u_0}(x_{i1} + x_{i2})\right) \tag{4}$$

$$\lambda_2 = P(X|\mathrm{H}_1) = \prod_{i=1}^{N} \frac{1}{\Gamma^2(L)}\left(\frac{L^2}{u_1 u_2}\right)^{L} x_{i1}^{L-1} x_{i2}^{L-1} \exp\left(-L\left(\frac{x_{i1}}{u_1} + \frac{x_{i2}}{u_2}\right)\right) \tag{5}$$

The likelihood ratio, λ, is obtained by combining equations (4) and (5):

$$\lambda = \frac{P(X|\mathrm{H}_1)}{P(X|\mathrm{H}_0)} = \left(\frac{u_0^2}{u_1 u_2}\right)^{LN} \exp\left(-L\left(\frac{\sum_{i=1}^{N} x_{i1}}{u_1} + \frac{\sum_{i=1}^{N} x_{i2}}{u_2} - \frac{\sum_{i=1}^{N} x_{i1}}{u_0} - \frac{\sum_{i=1}^{N} x_{i\,2}}{u_0}\right)\right) \tag{6}$$

Let $\eta_1 = \frac{1}{N}\sum_{i=1}^{N} x_{i1}$, $\eta_2 = \frac{1}{N}\sum_{i=1}^{N} x_{i2}$, then the ratio can be expressed as

$$\lambda = \frac{P(X|\mathrm{H}_1)}{P(X|\mathrm{H}_0)} = \left(\frac{u_0^2}{u_1 u_2}\right)^{LN} \exp\left(-NL\left(\frac{\eta_1}{u_1} + \frac{\eta_2}{u_2} - \frac{\eta_1}{u_0} - \frac{\eta_2}{u_0}\right)\right) \tag{7}$$

From a maximum likelihood estimation, it is easy to get the estimations of u_0, u_1 and u_2 with $\hat{u}_0 = \arg\max_{(u_1,u_2)}(\lambda_1)$ and $(\hat{u}_1, \hat{u}_2) = \arg\max_{(u_1,u_2)}(\lambda_2)$:

$$\begin{cases} \hat{u}_0 = \frac{1}{2N}\sum_{i=1}^{N}(x_{i1} + x_{i2}) = \frac{1}{2}(\eta_1 + \eta_2) \\ (\hat{u}_1, \hat{u}_2) = \left(\frac{1}{N}\sum_{i=1}^{N} x_{i1}, \frac{1}{N}\sum_{i=1}^{N} x_{i2}\right) = (\eta_1, \eta_2) \end{cases} \tag{8}$$

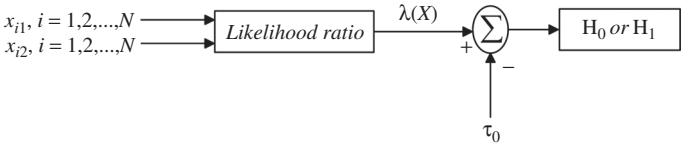

Figure 1. SAR change detection scheme based on a likelihood ratio of SAR images.

Thus, equation (7) can be expressed as follows:

$$\lambda = \frac{P(x|\mathrm{H}_1)}{P(x|\mathrm{H}_0)} = \left(\frac{(\eta_1+\eta_2)^2}{4\eta_1\eta_2}\right)^{LN} \exp(0) \underset{\mathrm{H}_0}{\overset{\mathrm{H}_1}{\gtrless}} \tau_0 \tag{9}$$

Figure 1 shows the scheme of change detection based on SAR statistical properties.

Simplification of equation (9) results in

$$\eta = \frac{\eta_1}{\eta_2} + \frac{\eta_2}{\eta_1} \underset{\mathrm{H}_0}{\overset{\mathrm{H}_1}{\gtrless}} 4\tau_0^{\frac{1}{LN}} - 2 = \tau \tag{10}$$

The expression $\eta = (\eta_1/\eta_2) + (\eta_2/\eta_1)$ is the new change detection measure, which is a simplified form of the likelihood ratio of the SAR intensity images. The symbol τ is the new threshold for change detection and η_k, $k = 1, 2$, are the average values in the sub-homogenous areas of the master and slave SAR images at the same location, respectively. To minimize computational requirements, small windows are used to avoid the necessity of searching for homogenous areas. It is noted that for 8-bit data, when η_1 equals η_2, η achieves its minimum value $\eta_{\min} = 2$. Therefore, we map η to η' with the range between 0 and 255. If there is no obvious change identified, then η' will be close to 0. Then a threshold is automatically chosen in this range based on the histogram of η'.

3. Results and analysis

A pair of European remote sensing satellite (ERS-2) SAR images and a pair of airborne SAR images are used to test the proposed change detection measure.

3.1 *ERS-2 SAR images*

Figure 2(*a*) and 2(*b*) shows two co-registered C-band SAR images after radiometric calibration acquired by ERS-2 over the city of Bern, Switzerland, on 20 April and 25 May 1999. The pixel size of the images is about 12.5 m. Flooding over the farmland, evident in figure 2(*b*), is mapped as the reference image with a visual interpretation in figure 2(*c*).

For the Bern data set, residual data were calculated using a 3 × 3 window, which was assumed to represent a homogenous area. The normalized histogram and its local amplification of the residual data are shown in figure 3(*a*) and 3(*b*). The single, sharp peak of the histogram is assumed to represent the unchanged part of the image, and the long tail of the histogram the changed part of the image. Since the unchanged pixels are very close to 0 and concentrated in the narrow peak, the value of the transitional

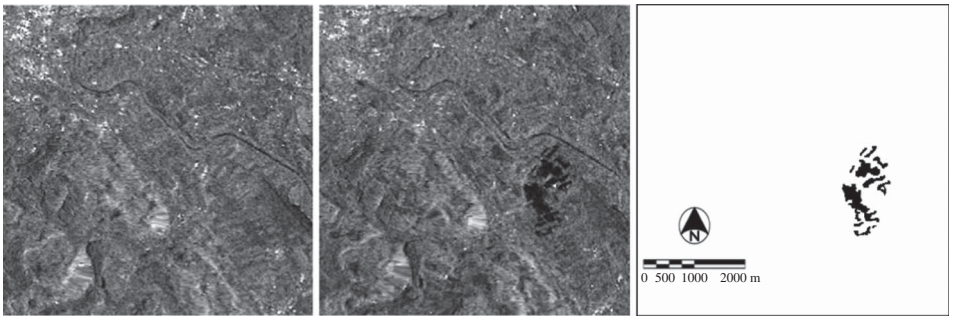

(*a*) (*b*) (*c*)

Figure 2. A pair of ERS-2 SAR images of Bern, Switzerland: (*a*) before and (*b*) after floods. (*c*) Reference image of change (represented by dark pixels).

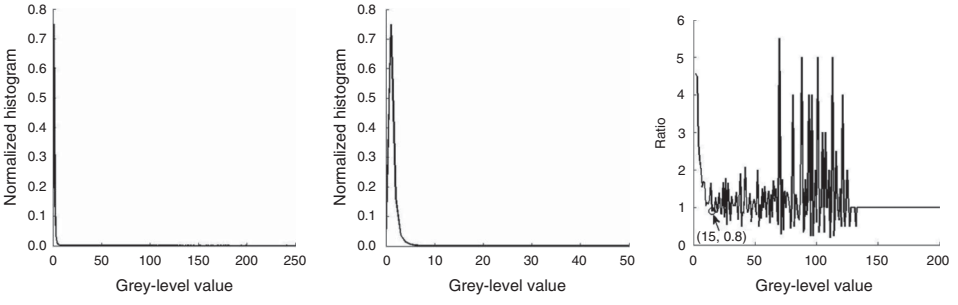

(*a*) (*b*) (*c*)

Figure 3. (*a*) Normalized histogram and (*b*) the local amplification of residual data from the Bern data set. (*c*) The ratio curve of the histogram and the first point with the ratio under 1.0 are taken as the threshold for change detection.

point between the peak and the tail can be chosen as the threshold when the histogram curve changes from steep to smooth. The ratios of the histogram at two adjacent grey-level values on the right side of the peak can be used to find the appropriate threshold. The first point with a ratio less than 1.0 is taken as the transitional point. After that point, the histogram enters into an oscillating state and the ratios fluctuate randomly around 1.0. Figure 3(*c*) is the ratio curve of the histogram. The first point with the ratio less than 1.0 is marked with a circle and its value is 15.

Figure 4(*a*) is the residual data before thresholding and (*b*) is the result of the change detection with the selected threshold, which corresponds well with the reference image.

Since log-ratio is a widely used measure in SAR change detection (Bazi *et al.* 2005, Bovolo and Bruzzone 2005), this letter compares the change detection results with a supervised manual trial-and-error procedure (MTEP) based on a log-ratio detector, which consists of finding the threshold value that minimizes the overall errors, and an unsupervised change detection with Kittler–Illingworth (KI) threshold selection based on general Gaussian (GG) model and the log-ratio detector (Bazi *et al.* 2005). Table 1 lists the change detection results, the overall error and the kappa coefficient to evaluate these methods. The kappa coefficients and overall errors show that the proposed method is better than that of the GG method and is very close to the result of MTEP.

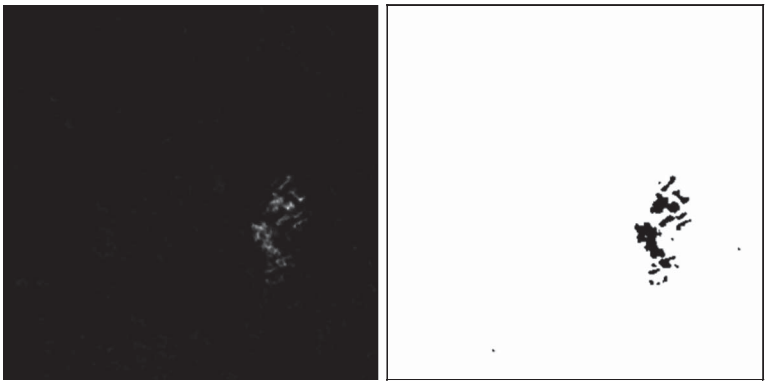

(*a*) (*b*)

Figure 4. (*a*) The residual data with the proposed change detection measure applied to the data shown in figure 2. (*b*) The change detection result after thresholding high values as changes and mapping them to black pixels.

Table 1. Results achieved by the proposed methods, MTEP and GG method (Bern SAR data set).

	Correctly identified changed pixels	Correctly identified unchanged pixels	Unchanged pixels classified as changed	Changed pixels classified as unchanged	Overall error	Kappa coefficient
MTEP	1210	127,259	140	272	412	0.853
GG method	1349	126,950	449	133	582	0.820
Proposed method	1165	127,288	111	317	428	0.843

3.2 *High-resolution airborne SAR images*

Figure 5(*a*) and 5(*b*) shows two X-band airborne SAR intensity images acquired over a field in Beijing, China, on 4 and 6 April 2004. The pixel size of the images is 0.5 m. The local incident angle was approximately 35°, and the flight azimuth approximately 75°. The numbers and positions of the vehicles on the field were different during the two data acquisition dates. These data sets were only approximately co-registered, with a registration error of about 1–2 pixels. Figure 5(*c*) is the ground change reference image with a visual interpretation.

Since notable speckle noise is present in these two images, a Frost filter with a 3×3 window was applied four times before the change detection operation, which resulted in a good trade-off between noise reduction and degradation of the spatial details of the data. Then the same 3×3 windows were used to replace the homogenous areas to acquire the residual data with the proposed change detection measure. Figure 6(*a*) and 6(*b*) shows the histogram and its local amplification of the residual data, and (*c*) is the ratio curve of the histogram. The grey-level value 18 was selected as the threshold value with the same method in the former experiment.

Figure 7(*a*) is the residual data before thresholding and (*b*) is the result of the change detection with the selected threshold, which also corresponds well with the ground reference image.

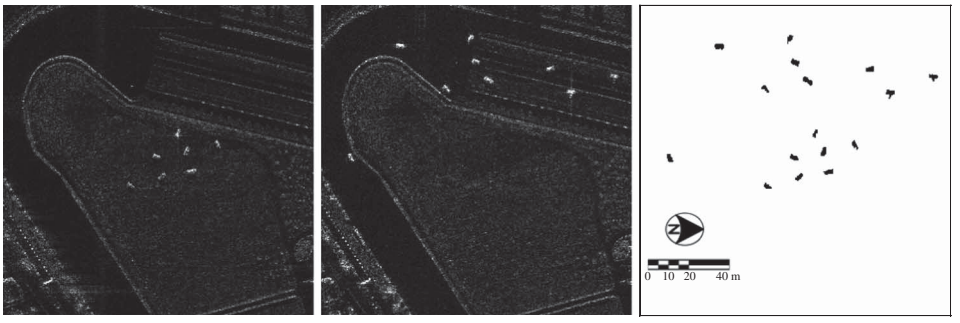

(*a*) (*b*) (*c*)

Figure 5. (*a*) and (*b*) A pair of high-resolution airborne SAR images with different vehicle distributions acquired 2 days apart. (*c*) Reference image of change (represented by dark pixels).

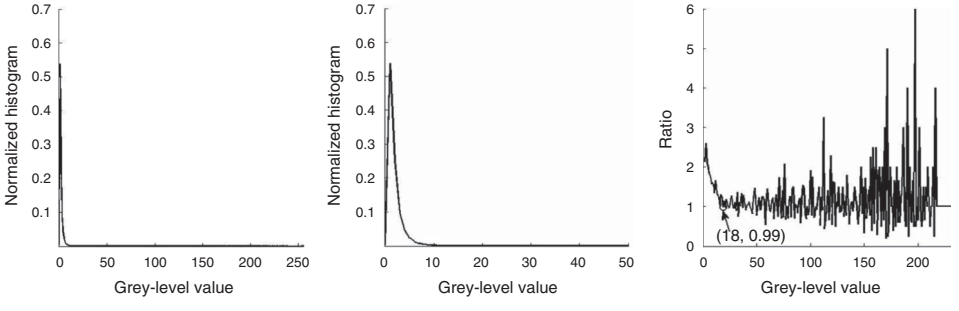

(*a*) (*b*) (*c*)

Figure 6. (*a*) Normalized histogram and (*b*) the local amplification of residual data from the airborne SAR data set. (*c*) The ratio curve of the histogram and the first point with the ratio under 1.0 are taken as the threshold for change detection.

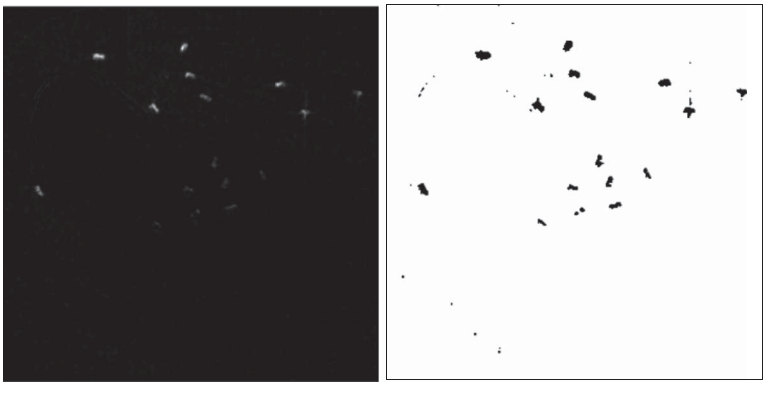

(*a*) (*b*)

Figure 7. (*a*) The residual data with the proposed change detection measure applied to the data shown in figure 5. (*b*) The change detection result after thresholding high values as changes and mapping them to black pixels.

Table 2. Results achieved by the proposed methods, MTEP and GG method (airborne SAR data set).

	Correctly identified changed pixels	Correctly identified unchanged pixels	Unchanged pixels classified as changed	Changed pixels classified as unchanged	Overall error	Kappa coefficient
MTEP	3263	804,911	550	1276	1826	0.780
GG method	3013	804,989	472	1526	2056	0.750
Proposed method	3795	803,899	1562	744	2306	0.766

Table 2 lists the evaluation of the change detection result. The kappa coefficients show that the proposed method is more accurate than the GG method and is very close to the result of MTEP. Though the overall error of the proposed method is higher than the benchmark methods, the number of correctly identified changed pixels is much larger than that of the other methods. Most of the false alarm pixels due to mis-registration potentially can be removed with a post change-classification procedure.

4. Conclusion

A change detection measure based on the likelihood ratio and statistical properties of SAR intensity images was developed in this letter. With the proposed change detection measure, the histogram of the residual image shows a single, sharp peak for the unchanged areas, which makes it straightforward to select a threshold to differentiate the changed pixels from the unchanged ones. The analyses of two SAR image pairs from different sensors with different resolutions show that the proposed measure can detect the change information from multi-temporal SAR images very well. The change detection results are very close to that from the MTEP and better than that from the unsupervised change detection method with KI thresholding based on the GG model.

Acknowledgements

The authors would like to thank the Chinese Scholarship Council for providing funds for this study. The authors are also thankful to Dr. Timothy Warner and the anonymous reviewers for their detailed comments, which helped very much to improve this letter.

References

Bazi, Y., Bruzzone, L. and Melgani, F., 2005, An unsupervised approach based on the generalized Gaussian model to automatic change detection in multitemporal SAR images. *IEEE Transactions on Geoscience and Remote Sensing*, **43**, pp. 874–887.

Bazi, Y., Bruzzone, L. and Melgani, F., 2006, Automatic identification of the number and values of decision thresholds in the log-ratio image for change detection in SAR images. *IEEE Geoscience and Remote Sensing Letters*, **3**, pp. 349–353.

Bovolo, F. and Bruzzone, L., 2005, A detail-preserving scale-driven approach to change detection in multitemporal SAR images. *IEEE Transactions on Geoscience and Remote Sensing*, **43**, pp. 2963–2972.

Bovolo, F. and Bruzzone, L., 2007, A split-based approach to unsupervised change detection in large-size multitemporal images: application to tsunami-damage assessment. *IEEE Transactions on Geoscience and Remote Sensing*, **45**, pp. 1658–1670.

Bruzzone, L. and Prieto, D.F., 2000, Automatic analysis of the difference image for unsupervised change detection. *IEEE Transactions on Geoscience and Remote Sensing*, **38**, pp. 1171–1182.

Chatelain, F. and Tourneret, J.-Y., 2007, Bivariate gamma distributions for multisensor SAR images. In *International Conference on Acoustics, Speech and Signal Processing*, 15–20 April, Honolulu, HI, pp. 1237–1240.

Conradsen, K., Nielsen, A.A., Schou, J. and Skriver, H., 2003, A test statistic in the complex Wishart distribution and its application to change detection in polarimetric SAR data. *IEEE Transactions on Geoscience and Remote Sensing*, **41**, pp. 4–19.

Coppin, P.R. and Bauer, M.E., 1996, Digital change detection in forest ecosystems with remote sensing imagery. *International Journal of Remote Sensing*, **13**, pp. 207–234.

Dekker, R.J., 1998, Speckle filtering in satellite SAR change detection imagery. *International Journal of Remote Sensing*, **19**, pp. 1133–1146.

Franceschetti, G. and Lanari, R., 1999, *Synthetic Aperture Radar Processing*, 1st Ed. (Boca Raton, FL: CRC Press LLC).

Inglada, J. and Mercier, G., 2007, A new statistical similarity measure for change detection in multitemporal SAR images and its extension to multiscale change analysis. *IEEE Transactions on Geoscience and Remote Sensing*, **45**, pp. 1432–1445.

Jha, C.S. and Unni, N.V.M., 1994, Digital change detection of forest conversion of a dry tropical Indian forest region. *International Journal of Remote Sensing*, **15**, pp. 2543–2552.

Makkeasorn, A., Chang, N.-B. and Li, J., 2009, Seasonal change detection of riparian zones with remote sensing images and genetic programming in a semi-arid watershed. *Journal of Environmental Management*, **90**, pp. 1069–1080.

Moser, G. and Serpico, S.B., 2006, Generalized minimum-error thresholding for unsupervised change detection from SAR amplitude imagery. *IEEE Transactions on Geoscience and Remote Sensing*, **44**, pp. 2972–2982.

Oliver, C. and Quegan, S., 2004, *Understanding Synthetic Aperture Radar Images*, 2nd Ed. (Raleigh, NC: SciTech Publishing Inc.).

Rignot, E.J.M. and Zyl, J.J.V., 1993, Change detection techniques for ERS-1 SAR data. *IEEE Transactions on Geoscience and Remote Sensing*, **31**, pp. 896–906.

Rogerson, P.A., 2002, Change detection thresholds for remotely sensed images. *Journal of Geographical Systems*, **4**, pp. 85–97.

Singh, A., 1989, Digital change detection techniques using remotely-sensed data. *International Journal of Remote Sensing*, **10**, pp. 989–1003.

Wang, Y. and Allen, T.R., 2008, Estuarine shoreline change detection using Japanese ALOS PALSAR HH and JERS-1 L-HH SAR data in the Albemarle-Pamlico Sounds, North Carolina, USA. *International Journal of Remote Sensing*, **29**, pp. 4429–4442.